

Photoelectrochemistry on Ru^{II}-2,2'-bipyridine-phosphonate-Derivatized TiO₂ with the I₃⁻/I⁻ and Quinone/Hydroquinone Relays. Design of Photoelectrochemical Synthesis Cells

Laurie A. Gallagher,[†] Scaffold A. Serron,[†] Xingu Wen,[†] Brooks J. Hornstein,[‡] D. M. Dattelbaum,[‡] J. R. Schoonover,[‡] and Thomas J. Meyer^{*‡}

Department of Chemistry, The University of North Carolina at Chapel Hill, CB #3290, Chapel Hill, North Carolina 27599-3290, and Los Alamos National Laboratory, Associate Director for Strategic Research, P.O. Box 1663, MS A127, Los Alamos, New Mexico 87545

Received August 25, 2004

Photocurrent measurements have been made on nanocrystalline TiO₂ surfaces derivatized by adsorption of a catalyst precursor, [Ru(tpy)(bpy(PO₃H₂)₂)(OH₂)]²⁺, or chromophore, [Ru(bpy)₂(bpy(PO₃H₂)₂)]²⁺ (tpy is 2,2':6',2''-terpyridine, bpy is 2,2'-bipyridine, and bpy(PO₃H₂)₂ is 2,2'-bipyridyl-4,4'-diphosphonic acid), and on surfaces containing both complexes. This is an extension of earlier work on an adsorbed assembly containing both catalyst and chromophore. The experiments were carried out with the I₃⁻/I⁻ or quinone/hydroquinone (Q/H₂Q) relays in propylene carbonate, propylene carbonate–water mixtures, and acetonitrile–water mixtures. Electrochemical measurements show that oxidation of surface-bound Ru^{III}–OH₂³⁺ to Ru^{IV}–O²⁺ is catalyzed by the bpy complex. Addition of aqueous 0.1 M HClO₄ greatly decreases photocurrent efficiencies for adsorbed [Ru(tpy)(bpy(PO₃H₂)₂)(OH₂)]²⁺ with the I₃⁻/I⁻ relay, but efficiencies are enhanced for the Q/H₂Q relay in both propylene carbonate–HClO₄ and acetonitrile–HClO₄ mixtures. The dependence of the incident photon-to-current efficiency (IPCE) on added H₂Q in 95% propylene carbonate and 5% 0.1 M HClO₄ is complex and can be interpreted as changing from rate-limiting diffusion to the film at low H₂Q to rate-limiting diffusion within the film at high H₂Q. There is no evidence for photoelectrochemical cooperativity on mixed surfaces containing both complexes with the IPCE response reflecting the relative surface compositions of the two complexes. These results provide insight into the possible design of photoelectrochemical synthesis cells for the oxidation of organic substrates.

Introduction

Nanocrystalline TiO₂ surface structures derivatized with polypyridyl complexes of Ru^{II} have provided the basis for a family of solar cells based on the photosensitized injection of an electron into the conduction band of TiO₂ and re-reduction of the oxidized form of the complex by the I⁻/I₃⁻ couple.^{1–8} We are interested in using this configuration and

the oxidative equivalents produced at the surface to produce photocurrents and carry out organic oxidations with visible light. In an earlier study, we reported on the photooxidation of the ligand-bridged assembly [(4,4'-CO₂H)₂bpy)(4,4'-Me₂-bpy)Ru^{II}_a(dpp)Ru^{II}_b(tpy)(H₂O)]⁴⁺ (((4,4'-CO₂H)₂bpy) is 2,2'-bipyridine-4,4'-dicarboxylic acid; 4,4'-Me₂bpy is 4,4'-dimethyl-2,2'-bipyridine; dpp is 2,3-bis(2-pyridyl)pyrazine; tpy is 2,2':6',2''-terpyridine).⁹ This assembly contained both surface-

* To whom correspondence should be addressed. E-mail: tjmeyer@lanl.gov.

[†] The University of North Carolina at Chapel Hill.

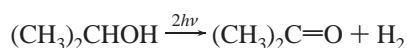
[‡] Los Alamos National Laboratory.

- (1) Garcia, C. G.; deLima, J. F.; Iha, N. Y. M. *Coord. Chem. Rev.* **2000**, *196*, 219.
- (2) Trammell, S. A.; Moss, J. A.; Yang, J. C.; Nakhle, B. M.; Slate, C. A.; Odobel, F.; Sykora, M.; Erickson, B. W.; Meyer, T. J. *Inorg. Chem.* **1999**, *38*, 3665.
- (3) Kalyanasundaram, K.; Grätzel, M. *Coord. Chem. Rev.* **1998**, *77*, 347.
- (4) Hagfeldt, A.; Grätzel, M. *Chem. Rev.* **1995**, *95*, 49–68.
- (5) Bignozzi, C. A.; Schoonover, J. R.; Scandola, F. *Prog. Inorg. Chem.* **1997**, *44*, 1.

- (5) Gerfin, T.; Grätzel, M.; Walder, L. *Prog. Inorg. Chem.* **1997**, *44*, 345.
- (6) Zakeeruddin, S. M.; Nazeeruddin, M. K.; Pechy, P.; Rotzinger, F. P.; Humphrey-Baker, R.; Kalyanasundaram, K.; Grätzel, M.; Shklover, V.; Haibach, T. *Inorg. Chem.* **1997**, *36*, 5937.
- (7) Heimer, T. A.; D'Arcangelis, S. T.; Farzad, F.; Stipkala, J. M.; Meyer, G. J. *Inorg. Chem.* **1996**, *35*, 5319.
- (8) (a) O'Regan, B.; Grätzel, M. *Nature* **1991**, *353*, 737–740. (b) Nazeeruddin, M. K.; Kay, A.; Rodicio, I.; Humphrey-Baker, E.; Müller, E.; Liska, P.; Vlachopoulos, N.; Grätzel, M. *J. Am. Chem. Soc.* **1993**, *115*, 6382.
- (9) Treadway, J. A.; Moss, J. A.; Meyer, T. J. *Inorg. Chem.* **1999**, *38*, 4386–4387.

adsorbed chromophore, $\text{Ru}^{\text{II}}_{\text{a}}$, and $\text{Ru}^{\text{II}}_{\text{b}}$, $\text{Ru}^{\text{II}}-\text{OH}_2^{2+}$, which is a precursor to $\text{Ru}^{\text{III}}-\text{OH}^{2+}$ and $\text{Ru}^{\text{IV}}=\text{O}^{2+}$. There is an extensive and well-defined oxidative chemistry of $\text{Ru}^{\text{IV}}=\text{O}^{2+}$ complexes toward organic substrates in solution.¹⁰

Visible photoexcitation of the molecular assembly in propylene carbonate resulted in photooxidation of $\text{Ru}^{\text{II}}_{\text{a}}$ to $\text{Ru}^{\text{III}}_{\text{a}}$, followed by sequential oxidation of $\text{Ru}^{\text{II}}_{\text{b}}-\text{OH}_2^{2+}$ to $\text{Ru}^{\text{III}}_{\text{b}}-\text{OH}^{2+}$ and then to $\text{Ru}^{\text{IV}}_{\text{b}}=\text{O}^{2+}$. Visible photoexcitation in 2-propanol led to oxidative dehydrogenation of the alcohol at the photoelectrode and formation of H_2 at the Pt electrode according to the equation:



We report here the results of a related study in which the separate components, chromophore and catalyst, are adsorbed separately on the same TiO_2 surface. In this case, photosensitized injection is followed by oxidation of hydroquinone (H_2Q) to quinone (Q). These studies reveal profoundly different effects of added water on photocurrents for the I_3^-/I^- and $\text{Q}/\text{H}_2\text{Q}$ couples as electron-transfer relays.

Experimental Section

Materials. High-purity propylene carbonate (99.7%) and perchloric acid (70%) were used as received from Aldrich. House-distilled water was purified further via a Barnstead E-Pure deionization system. Hydroquinone was purchased from Aldrich and recrystallized from water. Lithium iodide was used as received from Aldrich. Iodine was purchased from Aldrich and purified by sublimation. Titanium isopropoxide, DClO_4 (68%), and D_2O were used as received from Aldrich. Tin-doped indium oxide (20 Ω) electrodes were obtained from Delta Technologies, Ltd., Stillwater, MN, and were cleaned with ethanol and dried before use. All other common reagents were ACS grade and used without additional purification.

Syntheses. $[\text{Ru}(\text{tpy})(\text{bpy}(\text{PO}_3\text{H}_2)_2)(\text{OH}_2)](\text{ClO}_4)_2$. (tpy is 2,2':6',2''-terpyridine, and $\text{bpy}(\text{PO}_3\text{H}_2)_2$ is 2,2'-bipyridyl-4,4'-diphosphonic acid.) This salt was prepared according to a previously published method.¹¹

$[\text{Ru}(\text{bpy})_2(\text{bpy}(\text{PO}_3\text{H}_2)_2)](\text{Cl})_2$. This salt was prepared according to a previously reported synthesis for the hexafluorophosphate salt,² with the following modifications. A solution containing 100 mg of 2,2'-bipyridyl-4,4'-diphosphonic ethyl ester, $\text{bpy}(\text{PO}_3\text{Et}_2)_2$, and 145 mg of $\text{Ru}(\text{bpy})_2\text{Cl}_2$ in 12 mL of a degassed ethanol/water mixture (9:1/v:v) was heated at reflux under argon for 3 h. The reaction mixture was protected from ambient light. The progress of the reaction was monitored via UV-vis measurements at 458 nm. After 3 h, the solvent was removed by rotary evaporation and the residue was chromatographed on a silica gel column by using methanol saturated with NaCl as the eluent. The orange band, which moved very slowly, was collected and taken to dryness by rotary evaporation. The residue was extracted several times with methylene chloride. The methylene chloride solution was concentrated and dripped into ice-cold swirling ether, which caused the precipitation of a bright orange powder. This powder was collected by gravity filtration and chromatographed on a LH-20 size exclusion column. The main band was collected, and the solvent was concentrated and dripped into ice-cold swirling ether. The orange precipitate was

collected by gravity filtration. ^1H NMR spectroscopy at this stage in deuterated methylene chloride indicated that some hydrolysis of the phosphonated esters had occurred by the decrease in the ethyl resonances at ~ 1.5 ppm. To completely hydrolyze the esters, 20 mL of 3 M HCl was added and the solution was heated at reflux for 20 h. The solvent was removed by rotary evaporation. ^1H NMR spectroscopy in deuterated water indicated complete hydrolysis, as indicated by the disappearance of the ethyl resonances. In the ^{31}P NMR spectrum in deuterated water, using phosphoric acid as the reference, one resonance peak appeared at 8.229 ppm.

Electrode Preparation. Optically transparent TiO_2 nanoparticle films were prepared as described previously on conducting tin-doped indium oxide (ITO) surfaces.^{7,11} Films of nanoparticle TiO_2 (3–5 μm) were modified by adsorption of complexes from water or water/ethanol mixtures. The extent of surface loading was estimated by UV-visible measurement by the relationship $A(\lambda) = 1000\Gamma\epsilon(\lambda)$, where $A(\lambda)$ is the absorbance of the film, $\epsilon(\lambda)$ is the aqueous solution extinction coefficient for the complex in $\text{M}^{-1}\text{cm}^{-1}$, Γ is the surface coverage in mol cm^{-2} , and 1000 is the conversion factor between cm^3 and L. For $[\text{Ru}(\text{tpy})(\text{bpy}(\text{PO}_3\text{H}_2)_2)(\text{OH}_2)]^{2+}$ (**1**), $\epsilon(486) = 9600 \text{ M}^{-1}\text{cm}^{-1}$, and for $[\text{Ru}(\text{bpy})_2(\text{bpy}(\text{PO}_3\text{H}_2)_2)]^{2+}$ (**2**), $\epsilon(456) = 14\,000 \text{ M}^{-1}\text{cm}^{-1}$.^{2,11} Surfaces modified with both $[\text{Ru}(\text{tpy})(\text{bpy}(\text{PO}_3\text{H}_2)_2)(\text{OH}_2)]^{2+}$ and $[\text{Ru}(\text{bpy})_2(\text{bpy}(\text{PO}_3\text{H}_2)_2)]^{2+}$ were prepared by placing unmodified TiO_2 films into stock solutions containing different ratios of the complexes depending on the desired composition of the modified film. Surface adsorption at 25 $^\circ\text{C}$ in aqueous solution for **1** and **2** both follow the Langmuir isotherm with $K = 3 \times 10^5 \text{ M}^{-1}$ and $K = 2 \times 10^5 \text{ M}^{-1}$, respectively.^{11,12}

Measurements. UV-visible measurements were made with a HP-8452 diode array spectrometer. Cyclic voltammetry was performed by using a PAR 273 potentiostat with the standard three-electrode configuration in a two-compartment cell. The medium used was 0.1 M NaClO_4 in water. The reference electrode was saturated sodium chloride (SSCE), and the counter electrode was Pt.

X-ray photoelectron spectroscopy measurements (XPS) were conducted on a Perkin-Elmer Physical Electronics model 5400 spectrometer. A Mg $\text{K}\alpha$ X-ray source (400 W, 15 kV) was used with a hemispherical analyzer pass energy of 35.75 eV, and an angle of collection of 45 $^\circ$. Quantitative atomic ratios were calculated by using the instrumental relative sensitivity factors and integrated photoelectron peak areas.

Photocurrent measurements were performed as described elsewhere in a thin-layer, two-electrode cell.¹³ The counter electrode of the cell was a Pt foil sealed in a block of epoxy resin attached to a thick copper wire. The TiO_2 electrode was sandwiched against the Pt foil with a Parafilm spacer. Reductant solution was drawn into the cell by capillary action. The irradiation source was a 75 W xenon lamp coupled to a f4 matched monochromator with 1200 lines/in. gratings and powered by a PTI model LPS-220 Arc Lamp Supply. The light from the monochromator was then passed through two glass lenses. Light intensity was measured with an IL 500 radiometer. Currents were measured with a Keithley 6512 programmable electrometer.

Incident photon-to-current conversion efficiencies (IPCE) at each incident wavelength were calculated from eq 1.^{14,15}

$$\text{IPCE}(\lambda) = (1240 \text{ eV nm}) I_{\text{ph}} / \lambda P_0 \quad (1)$$

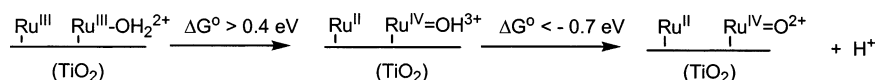
In eq 1, I_{ph} is the incident photocurrent density in mA/cm^2 , λ is the

(10) Huynh, M. H. V.; Meyer, T. J. *Inorg. Chem.* **2003**, *42*, 8140–8160.

(11) Gallagher, L. A.; Meyer, T. J. *J. Am. Chem. Soc.* **2001**, *123*, 5308–5312.

(12) Yang, J. C. Ph.D. Dissertation, University of North Carolina, Chapel Hill, NC, 2000.

Scheme 1



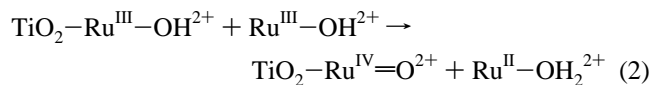
wavelength of the incident radiation in nm, and P_0 is the photon flux in mW/cm^2 . Photon flux was measured prior to IPCE experiments by using an IL1700, International Light, Inc. radiometer. Action spectra were recorded by making IPCE measurements on dye-sensitized films at 10 nm intervals between 400 and 600 nm.

Results

Surfaces modified by adsorption of $[\text{Ru}(\text{tpy})(\text{bpy}(\text{PO}_3\text{H}_2)_2)(\text{OH}_2)]^{2+}$ (**1**) ($\text{TiO}_2\text{-Ru}^{\text{III}}\text{-OH}_2^{2+}$) and $[\text{Ru}(\text{bpy})_2(\text{bpy}(\text{PO}_3\text{H}_2)_2)]^{2+}$ (**2**) ($\text{TiO}_2\text{-Ru}^{\text{II}}$) were stable over several days in aqueous solution, as shown by spectrophotometric measurements. Phosphonate binding to TiO_2 surfaces provides a stable linkage in acidic aqueous solution (in contrast to carboxylate binding) and in propylene carbonate.⁶

Maximum coverages of **1** and **2** in the TiO_2 thin films used here were $\sim 9 \times 10^{-8}$ and $\sim 7 \times 10^{-8}$ mol/cm^2 , respectively, as estimated by UV-visible spectroscopy. This corresponds to ~ 900 effective monolayers for $[\text{Ru}(\text{tpy})(\text{bpy}(\text{PO}_3\text{H}_2)_2)(\text{OH}_2)]^{2+}$ and ~ 700 for $[\text{Ru}(\text{bpy})_2(\text{bpy}(\text{PO}_3\text{H}_2)_2)]^{2+}$ based on the area of the surface and assuming a monolayer coverage of $\sim 1 \times 10^{-10}$ mol/cm^2 as estimated from van der Waals radii.^{16,17}

In a cyclic voltammogram in HClO_4 at $\text{pH} = 0.6$ for an ITO/ TiO_2 electrode fully loaded with $[\text{Ru}(\text{tpy})(\text{bpy}(\text{PO}_3\text{H}_2)_2)(\text{OH}_2)]^{2+}$, a single wave appears at $E_{1/2} \approx 800$ mV for the Ru(III/II) couple. Further oxidation to $\text{Ru}^{\text{IV}}\text{=O}^{2+}$ is not observed under these conditions, but a Ru(IV/III) wave was observed when a catalytic amount of $[\text{Ru}(\text{tpy})(\text{bpy})(\text{OH}_2)]^{2+}$ ($\geq 4.3 \times 10^{-5}$ M) was added to the external solution as noted previously.¹⁸ Oxidation to Ru(IV) is hindered on the surface because the potential for the direct oxidation of $\text{Ru}^{\text{III}}\text{-OH}_2^{2+}$ to $\text{Ru}^{\text{IV}}\text{=OH}^{3+}$ occurs > 1.4 V, which is past the solvent limit.¹⁹ Addition of the relay couple opens a surface pathway for oxidation by surface-solution disproportionation, eq 2, which is disfavored by 0.1 V.^{18,19}



Disproportionation is followed by oxidation of $\text{Ru}^{\text{II}}\text{-OH}_2^{2+}$ to $\text{Ru}^{\text{III}}\text{-OH}_2^{2+}$ at the electrode in solution and proton loss to give $\text{Ru}^{\text{III}}\text{-OH}_2^{2+}$.

The ratios of **1** to **2** on mixed surfaces of TiO_2 were determined by cyclic voltammetry by integrating the reductive component of the Ru(III/II) wave of the current-potential waveforms. A cyclic voltammogram in an aqueous solution of 0.1 M NaClO_4 ($\text{pH} \approx 6$) for a 1:1 ratio of **1** to **2** on a mixed surface is shown in Figure 1. The wave at $E_{1/2}$

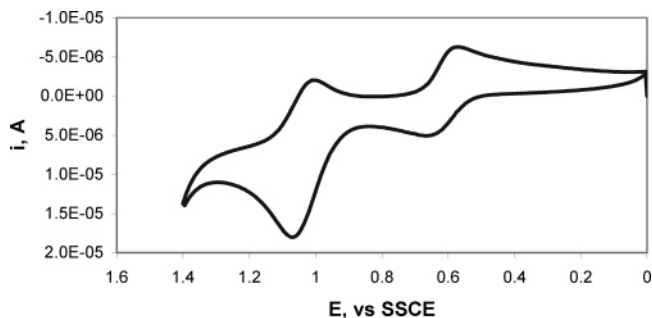


Figure 1. Cyclic voltammogram of a 50% $[\text{Ru}(\text{tpy})(\text{bpy}(\text{PO}_3\text{H}_2)_2)(\text{OH}_2)]^{2+}$ /50% $[\text{Ru}(\text{bpy})_2(\text{bpy}(\text{PO}_3\text{H}_2)_2)]^{2+}$ mixed surface in 0.1 M NaClO_4 ($\text{pH} \approx 6$). Scan rate is 5 mV/s, vs SSCE.

$= 620$ mV is the Ru(III/II) couple for $\text{TiO}_2\text{-Ru}^{\text{III}}\text{-OH}_2^{2+}$ / $\text{Ru}^{\text{II}}\text{-OH}_2^{2+}$, and the wave at $E_{1/2} = 1040$ mV is the Ru(III/II) couple for **2**. The Ru(IV/III) wave for adsorbed **1** would appear at ~ 720 mV,¹⁸ but, as noted above, it cannot be observed without the use of an external relay. The wave at $E_{1/2} = 1040$ mV arises from the adsorbed $[\text{Ru}^{\text{III}}(\text{bpy})_2(\text{bpy}(\text{PO}_3\text{H}_2)_2)]^{2+}$ / $[\text{Ru}^{\text{II}}(\text{bpy})_2(\text{bpy}(\text{PO}_3\text{H}_2)_2)]^{2+}$ couple.

The enhanced oxidative peak current for the wave at 1040 mV arises from the oxidative component of the “missing” $\text{Ru}^{\text{IV}}\text{=O}^{2+}/\text{Ru}^{\text{III}}\text{-OH}_2^{2+}$ wave. This is an important observation because it shows that further oxidation of $\text{TiO}_2\text{-Ru}^{\text{III}}\text{-OH}_2^{2+}$ to $\text{TiO}_2\text{-Ru}^{\text{IV}}\text{=O}^{2+}$ does occur on surfaces containing coadsorbed $\text{TiO}_2\text{-Ru}^{\text{III}}$.

A possible mechanism for this reaction involving electron transfer followed by proton transfer is illustrated in Scheme 1. Initial electron transfer is disfavored by $\Delta G_o > 0.4$ eV, while proton transfer is favored by $\Delta G_o < -0.7$ eV at $\text{pH} = 6$. For the net reaction, $\text{TiO}_2\text{-Ru}^{\text{III}} + \text{TiO}_2\text{-Ru}^{\text{III}}\text{-OH}_2^{2+} \rightarrow \text{TiO}_2\text{-Ru}^{\text{II}} + \text{TiO}_2\text{-Ru}^{\text{IV}}\text{=O}^{2+} + \text{H}^+$ at $\text{pH} = 6$, $\Delta G^\circ = -0.3$ eV.

A $\text{TiO}_2\text{-Ru}^{\text{IV}}\text{=O}^{2+}/\text{TiO}_2\text{-Ru}^{\text{III}}\text{-OH}_2^{2+}$ reduction wave at ~ 720 mV does not appear following the oxidative scan through the $\text{TiO}_2\text{-Ru}^{\text{III}}/\text{TiO}_2\text{-Ru}^{\text{II}}$ wave in Figure 1. A wave for the $\text{TiO}_2\text{-Ru}^{\text{III}}\text{-OH}_2^{2+}/\text{TiO}_2\text{-Ru}^{\text{II}}\text{-OH}_2^{2+}$ couple does appear at 620 mV, which “tails” noticeably to more reductive potentials on the cathodic side, Figure 1. Catalyzed reduction of $\text{TiO}_2\text{-Ru}^{\text{IV}}\text{=O}^{2+}$ to $\text{TiO}_2\text{-Ru}^{\text{III}}\text{-O}^+$ by the reaction $\text{TiO}_2\text{-Ru}^{\text{II}} + \text{TiO}_2\text{-Ru}^{\text{IV}}\text{=O}^{2+} \rightarrow \text{TiO}_2\text{-Ru}^{\text{III}} + \text{TiO}_2\text{-Ru}^{\text{III}}\text{-O}^+$ is highly nonspontaneous with $\Delta G^\circ > 0.8$ eV.¹⁸ The reduction mechanism on the surface may be complex with slow $\text{Ru}^{\text{IV}}\text{=O}^{2+}$ reduction to $\text{Ru}^{\text{III}}\text{-O}^+$ affecting the reductive waveform. Subsequent rapid protonation and further reduction of $\text{Ru}^{\text{III}}\text{-OH}_2^{2+}$ to $\text{Ru}^{\text{II}}\text{-OH}_2^{2+}$ would

- (13) Moss, J. A. Ph.D. Dissertation, University of North Carolina, Chapel Hill, 1997.
 (14) Heimer, T. A.; Heilweil, E. J.; Bignozzi, C. A.; Meyer, G. J. *J. Phys. Chem. B* **2000**, *104*, 4256.
 (15) Argazzi, R.; Bignozzi, C. A.; Heimer, T. A.; Castellano, F. N.; Meyer, G. J. *Inorg. Chem.* **1994**, *33*, 5741.
 (16) Meyer, T. J.; Meyer, G. J.; Pfenning, B. W.; Schoonover, J. R.; Timpson, C. J.; Wall, J. F.; Kobusch, C.; Chen, X.; Peek, B. M.; Wall, C. G.; Ou, W.; Erickson, B. W.; Bignozzi, C. A. *Inorg. Chem.* **1994**, *33*, 3952.
 (17) Trammell, S. A.; Meyer, T. J. *J. Phys. Chem. B* **1999**, *103*, 104–107.
 (18) Trammell, S. A.; Wimbish, J. C.; Odobel, F.; Gallagher, L. A.; Narula, P. M.; Meyer, T. J. *J. Am. Chem. Soc.* **1998**, *120*, 13248.
 (19) Binstead, R. A.; Meyer, T. J. *J. Am. Chem. Soc.* **1987**, *109*, 3287.

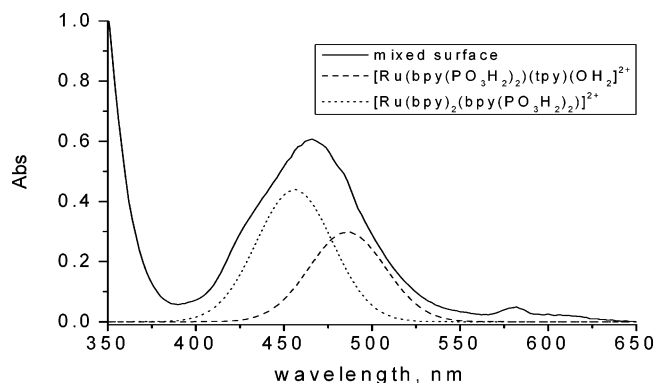


Figure 2. UV-visible spectrum in water of a 50% [Ru(tpy)(bpy(PO₃H₂))(OH₂)]²⁺/50% [Ru(bpy)₂(bpy(PO₃H₂))]²⁺ mixed surface.

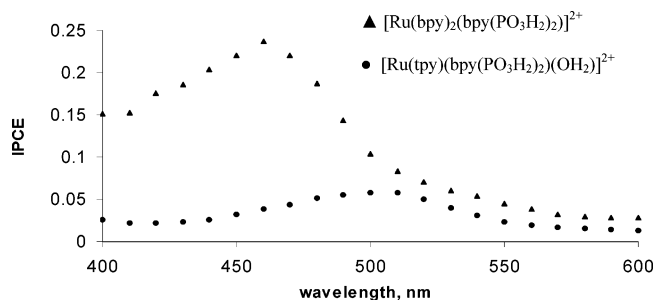


Figure 3. IPCE(λ) versus λ spectra for TiO₂ absorbed [Ru(tpy)(bpy(PO₃H₂))(OH₂)]²⁺ (**1**) and [Ru(bpy)₂(bpy(PO₃H₂))]²⁺ (**2**) in propylene carbonate with the I⁻/I₃⁻ redox relay.

complete the conversion of TiO₂-Ru^{IV}=O²⁺ to TiO₂-Ru^{II}-OH₂²⁺.

The visible absorption spectrum of a 1:1 mixed surface, with the composition determined electrochemically, is shown in Figure 2. In this spectrum, the visible MLCT absorption bands for (**1**) $\lambda_{\text{max}} = 486$ nm and (**2**) $\lambda_{\text{max}} = 456$ nm are badly overlapped.^{2,11} As shown in Figure 2, the mixed surface spectrum is essentially the sum of the spectra of the separate components.

Incident photon-to-current conversion efficiency (IPCE) measurements were conducted and referenced to [Ru(bpy)₂(bpy(PO₃H₂))]²⁺ adsorbed to TiO₂ on tin-doped indium oxide electrodes with the I₃⁻/I⁻ couple in propylene carbonate as reported previously. An IPCE value of ~23% was measured at 470 nm for this surface dye.² Action spectra, IPCE(λ) versus λ , for films containing either TiO₂-Ru^{II}-OH₂²⁺ or TiO₂-Ru^{II} matched closely the absorption spectra of the adsorbed dyes. IPCE values for TiO₂-Ru^{II}-OH₂²⁺ were only ~25% of those for TiO₂-Ru^{II}. Part of the decrease is due to the decrease in absorptivity of ~70% for the aqua complexes with a slight shift to the red for both cases. Action spectra for both are shown in Figure 3.

The IPCE values decrease dramatically with added aqueous 0.1 M HClO₄ with the I₃⁻/I⁻ couple as redox carrier for both **1** and **2**. This effect is illustrated for TiO₂-Ru^{II}-OH₂ (**1**) in Figure 4A with the IPCE value at 510 nm decreasing by ~40% with the addition of 1% aqueous 0.1 M HClO₄ by volume. The effect is reversible with the photocurrent restored in a dry propylene carbonate solution.

Hydroquinone as Reductant. With the quinone/hydroquinone couple rather than the I₃⁻/I⁻ couple as relay, a

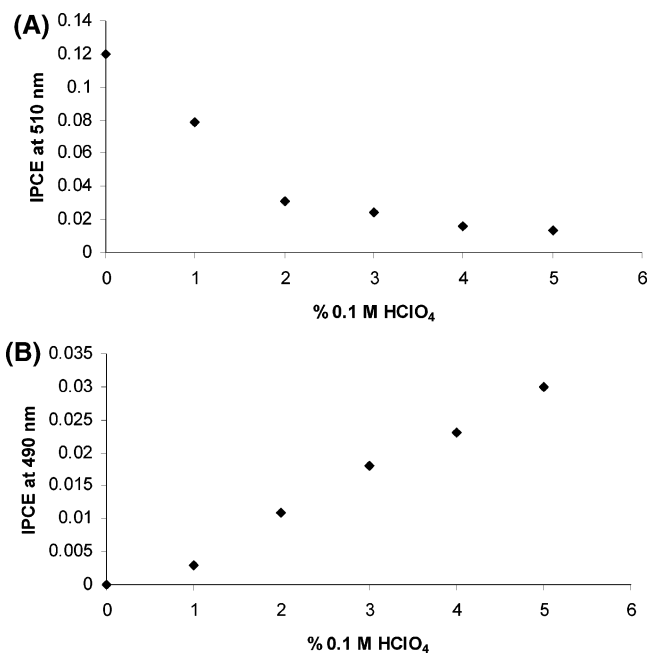
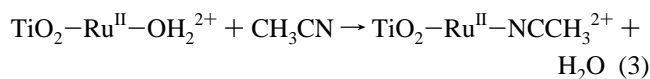


Figure 4. (A) IPCE versus % 0.1 M HClO₄ in propylene carbonate for TiO₂-Ru^{II}-OH₂²⁺ (**1**) with the I₃⁻/I⁻ relay couple. (B) As in (A) with the Q/H₂Q relay couple.

different behavior was observed with added aqueous acid. In films of **2**, with added 0.1 M HClO₄, photocurrents were initially ~10 \times smaller than those observed with I₃⁻/I⁻, but currents decreased over time to nearly zero in less than an hour. UV-visible and electrochemical measurements revealed no significant change in the amount or nature of the adsorbed complex.

For **1** on TiO₂, addition of increasing amounts of aqueous HClO₄ caused a decrease in IPCE with the I₃⁻/I⁻ relay as for **2**. By contrast, with the Q/H₂Q carrier couple, IPCE values increased upon addition of 0.1 M HClO₄. As shown in Figure 4B, a maximum IPCE value of ~3% was reached at the miscibility limit of 5% added aqueous HClO₄ and 0.1 M H₂Q. Experiments were also performed in 5% 0.1 M DClO₄ in propylene carbonate with both 1 \times 10⁻³ M and 0.1 M hydroquinone. There was no discernible isotope effect under either set of conditions. In contrast to **2**, with the Q/H₂Q relay and added HClO₄, IPCE values for **1** were stable over extended periods (hours). The variation in IPCE(λ) with [H₂Q] in 95% propylene carbonate and 5% 0.1 M HClO₄ is shown in Figure 5.

Because of the higher solubility of H₂Q in acetonitrile as compared to propylene carbonate, IPCE measurements were also performed with H₂Q in acetonitrile-water mixtures. There is a potential complication in this medium from substitution of coordinated H₂O by CH₃CN, eq 3.



That substitution occurs in pure acetonitrile was confirmed by IPCE measurements. After exposure of **1** to acetonitrile, the maximum in the IPCE(λ) versus λ spectrum shifted from the characteristic maximum for the aqua complex at 490 nm

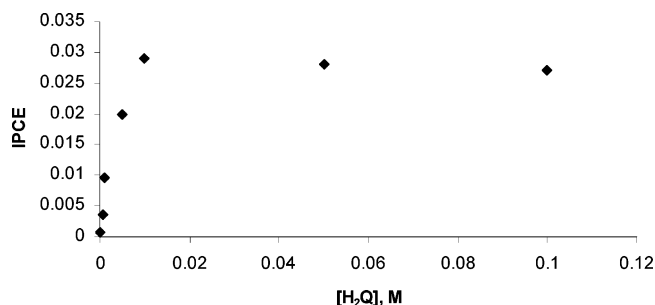


Figure 5. Variations in IPCE(λ) of $\text{TiO}_2\text{-Ru}^{\text{II}}\text{-OH}_2^{2+}$ (**1**) with excitation at 520 nm as a function of hydroquinone concentration in 95% propylene carbonate and 5% 0.1 M HClO_4 .

to that of the CH_3CN complex at 470 nm, and the peak current decreased by a factor of ~ 2 .

The influence of aqueous 0.1 M HClO_4 on the IPCE for $\text{TiO}_2\text{-Ru-OH}_2^{2+}$ with added Q/ H_2Q in acetonitrile is complex, but photocurrents increased with added acid up to 30% 0.1 M HClO_4 , reaching a maximum of ~ 0.1 .

Mixed Surfaces. Measurements were also made on surface mixtures of 1:3, 1:1, and 3:1 $\text{TiO}_2\text{-Ru}^{\text{II}}\text{-OH}_2^{2+}:\text{TiO}_2\text{-Ru}^{\text{II}}$. Photocurrents for the mixed surfaces with I_3^-/I^- in propylene carbonate were, within experimental error, the sum of the fractional surface coverages, χ_a and χ_b , weighted by the IPCE(λ) values for the pure surfaces, eq 4.

$$\text{IPCE}_{\text{mixed surface}} = \chi_a \text{IPCE}_a(\lambda) + \chi_b \text{IPCE}_b(\lambda) \quad (4)$$

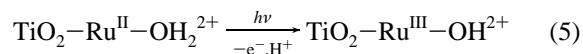
Discussion

The goal of this work was to explore the photocurrent characteristics of mixed TiO_2 surfaces containing the relatively efficient photoinjector $[\text{Ru}(\text{bpy})_2(\text{bpy}(\text{PO}_3\text{H}_2)_2)]^{2+}$ (**2**) and the redox catalyst precursor, $[\text{Ru}(\text{tpy})(\text{bpy}(\text{PO}_3\text{H}_2))(\text{OH}_2)]^{2+}$ (**1**). On surfaces containing only the latter, oxidation to $[\text{Ru}^{\text{III}}(\text{tpy})(\text{bpy}(\text{PO}_3\text{H}_2))(\text{OH})]^{2+}$ occurs, but further oxidation to $[\text{Ru}^{\text{IV}}(\text{tpy})(\text{bpy}(\text{PO}_3\text{H}_2))(\text{O})]^{2+}$ occurs only with an added redox carrier in the external solution. The $\text{p}K_a$ for the analogue $[\text{Ru}^{\text{III}}(\text{tpy})(\text{bpy})(\text{OH}_2)]^{3+}$ is 1.7 in solution, and for $[\text{Ru}^{\text{II}}(\text{tpy})(\text{bpy})(\text{OH}_2)]^{2+}$ it is 9.7.²⁰

There is an extensive catalytic and stoichiometric oxidation chemistry of $\text{Ru}^{\text{IV}}=\text{O}^{2+}$ polypyridyl complexes.^{10,19,21–33} We

recently showed that this reactivity is maintained in $[\text{Ru}^{\text{IV}}(\text{tpy})(\text{bpy}(\text{PO}_3\text{H}_2))(\text{O})]^{2+}$ adsorbed to TiO_2 .¹¹

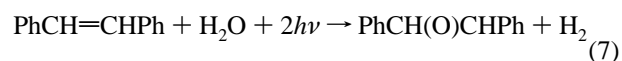
The $\text{Ru}^{\text{II}}\text{-OH}_2^{2+}$ form of **1** is a typical metal-to-ligand charge-transfer (MLCT) chromophore with $\lambda_{\text{max}} = 486$ in water adsorbed to TiO_2 . However, the intense MLCT visible light absorptivity is lost upon oxidation to $\text{Ru}^{\text{III}}\text{-OH}^{2+}$. As shown in eq 5, this provides a basis for the usual one-photon, one-electron injection cycle on TiO_2 , which, when coupled with the I_3^-/I^- relay couple, provides the basis for a photoelectrochemical cell. There is an earlier example of a ruthenium aqua complex as a sensitizer on TiO_2 in a dye-sensitized solar cell based on adsorbed *cis*- $[\text{Ru}^{\text{II}}(4,4'-(\text{CO}_2\text{H})_2\text{-bpy})_2(\text{OH}_2)]^{2+}$.³⁴



Because of the loss of MLCT absorption upon oxidation to $\text{TiO}_2\text{-Ru}^{\text{III}}\text{-OH}^{2+}$, an efficient light harvesting ability by photoinjection is lost in the once-oxidized form, and there is no direct sensitized pathway for the production of the catalytically more interesting $\text{Ru}^{\text{IV}}=\text{O}^{2+}$ form.

We have reported on the existence of relatively facile cross-surface electron transfer between polypyridyl complexes adsorbed on TiO_2 .³⁵ Cross-surface electron transfer could create a possible indirect route to $\text{TiO}_2\text{-Ru}^{\text{IV}}=\text{O}^{2+}$. This is shown in Scheme 2 and involves excitation and injection by adsorbed **2** followed by cross-surface electron transfer and oxidation of $\text{TiO}_2\text{-Ru}^{\text{III}}\text{-OH}^{2+}$ to Ru^{IV} . From redox potential measurements at $\text{pH} = 6.0$, this reaction is favored with $\Delta G^\circ = -0.3$ eV.

The formation of $\text{Ru}^{\text{IV}}=\text{O}^{2+}$ on the surface would open the possibility of using the photoelectrochemically produced oxidative equivalents to perform organic oxidations through two-electron transformations. In many organic oxidations, protons are released, which, in an aqueous environment, provides a low overvoltage route to H_2 at the cathode. If this strategy were successful, it would open the possibility of using the sensitized TiO_2 photoelectrochemical cell approach for creating a family of photoelectrochemical synthesis cells with H_2 produced at the cathode and net organic oxidations such as alcohol oxidation and epoxidation of olefins, eqs 6 and 7, at the anode.



As mentioned in the Introduction, this approach has been proven in concept for the dehydrogenation of 2-propanol by using an adsorbed, ligand-bridged assembly containing separate chromophore and catalytic functions.⁹ The results described here were designed to explore this possibility based on adsorption of separate chromophore and catalyst complexes on the same TiO_2 surface.

(20) Takeuchi, K. J.; Thompson, M. S.; Pipes, D. W.; Meyer, T. J. *Inorg. Chem.* **1984**, *23*, 1845.

(21) Stultz, L. K.; Huynh, M. V.; Binstead, R. A.; Curry, M.; Meyer, T. J. *J. Am. Chem. Soc.* **2000**, *122*, 5984.

(22) Catalano, V. J.; Heck, R. A.; Immoos, C. E.; Öhman, A.; Hill, M. G. *Inorg. Chem.* **1998**, *37*, 2150.

(23) Stultz, L. K.; Binstead, R. A.; Reynolds, M. S.; Meyer, T. J. *J. Am. Chem. Soc.* **1995**, *117*, 2520.

(24) Binstead, R. A.; McGuire, M. E.; Dovletoglou, A.; Seok, W. K.; Roecker, L. E.; Meyer, T. J. *J. Am. Chem. Soc.* **1992**, *114*, 173.

(25) Muller, J. G.; Acquaye, J. H.; Takeuchi, K. J. *Inorg. Chem.* **1992**, *31*, 4552.

(26) Leung, W.-H.; Che, C.-M. *J. Am. Chem. Soc.* **1989**, *111*, 8812.

(27) Seok, W. K.; Meyer, T. J. *J. Am. Chem. Soc.* **1988**, *110*, 7358.

(28) Roecker, L.; Meyer, T. J. *J. Am. Chem. Soc.* **1987**, *109*, 746.

(29) Gilbert, J.; Roecker, L.; Meyer, T. J. *Inorg. Chem.* **1987**, *26*, 1126.

(30) Roecker, L.; Meyer, T. J. *J. Am. Chem. Soc.* **1986**, *108*, 4066.

(31) Thompson, M. S.; Meyer, T. J. *J. Am. Chem. Soc.* **1982**, *104*, 5070.

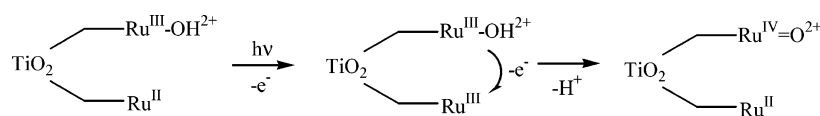
(32) Thompson, M. S.; Meyer, T. J. *J. Am. Chem. Soc.* **1982**, *104*, 4106.

(33) Moyer, B. A.; Sipe, B. K.; Meyer, T. J. *Inorg. Chem.* **1981**, *20*, 1475.

(34) Liska, P.; Vlachopoulos, N.; Nazeeruddin, M. K.; Comte, P.; Grätzel, M. *J. Am. Chem. Soc.* **1988**, *110*, 3686.

(35) Trammell, S. A.; Meyer, T. J. *J. Phys. Chem. B* **1999**, *103*, 104–107.

Scheme 2



I₃⁻/I⁻ Relay. Light absorption by TiO₂-Ru^{II}-OH₂²⁺ (**1**) on TiO₂ in propylene carbonate with the I₃⁻/I⁻ relay leads to sustained photocurrents, but IPCE values are only ~25% of those for TiO₂-Ru^{II} (**2**) with excitation at their respective IPCE maxima, Figure 3. This may be due, at least in part, to the lower light absorptivity for the aqua complex and a relatively short excited-state lifetime for the MLCT excited state(s) of [Ru^{II}(tpy)(bpy(PO₃H₂)₂)(H₂O)]²⁺. There is no evidence for emission from the complex in solution.

The inclusion of water is important in maintaining the surface Ru=O²⁺/Ru-OH₂²⁺ couples and for providing a proton reservoir for reactions involving proton transfer. A few early experiments with nanocrystalline TiO₂ electrodes for dye-sensitized solar cells were performed in aqueous media.^{34,36,37} Although large IPCE values were once reported in aqueous media,^{34,36} there have been no additional reports under such conditions since 1993.³⁶ In a study by Nazeeruddin and co-workers, water was reported to lower the injection efficiencies of dye-sensitized electrodes,^{8b} although no explanation was offered for the effect.

Our IPCE results on both TiO₂-Ru^{II}-OH₂²⁺ and TiO₂-Ru^{II} with the I₃⁻/I⁻ carrier couple show that addition of aqueous 0.1 M aqueous HClO₄ decreases IPCE values incrementally with the effect leveling off past 3 vol %, Figure 4A for TiO₂-Ru^{II}-OH₂²⁺. There is no effect on the UV-visible spectrum of the adsorbed complexes in this medium, and the effect is reversible. We have not investigated the microscopic origin of the effect of water but conclude that it must be a medium effect. A possible role for small amounts of added water is selective solvation and its effect on the thermodynamics (and the electron-transfer reactivity) of the I₃⁻/I⁻ couple. Another could be its effect on the extent of ion association at the adsorbed redox sites.

Hydroquinone. The use of hydroquinone as reductant and the Q/H₂Q carrier couple was investigated as an example of an organic relay in place of I₃⁻/I⁻. Hydroquinone was used as a “supersensitizer”, during early studies of photoinjection on dye-sensitized planar semiconductor electrodes.³⁸ The difference in behavior between TiO₂-Ru^{II}-OH₂²⁺ and TiO₂-Ru^{II} with the Q/H₂Q couple is striking.

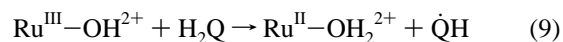
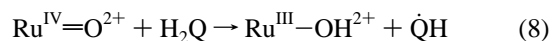
With I₃⁻/I⁻ and TiO₂-Ru^{II} films in propylene carbonate, the maximum IPCE is 23%.² With hydroquinone as reductant, initial IPCE values are lower by nearly a factor of 10. Further exposure to light in the presence of hydroquinone over a period of ~1 h, under standard cell operating conditions, leads to permanent loss of an IPCE response.

To ascertain if the integrity of adsorbed [Ru(bpy)₂(bpy(PO₃H₂)₂)]²⁺ had been compromised, both absorbance and

cyclic voltammetric measurements were performed. In UV-visible spectra, the characteristic MLCT band for [Ru(bpy)₂(bpy(PO₃H₂)₂)]²⁺ at λ_{max} = 460 nm was observed with no apparent loss in absorbance due to desorption. In cyclic voltammograms, a single wave for the Ru(III/II) couple appeared at E_{1/2} = 1010 mV, only slightly shifted from E_{1/2} = 1040 mV obtained before the photocurrent experiments. To check the integrity of the TiO₂ after the photocurrent experiments with hydroquinone, films were examined by XPS before and after the experiment. No change in the Ti^{III}/Ti^{IV} ratio was observed, and there was also no sign of carbon buildup on the films. None of these experimental probes gave insight into the origin of the loss of photoelectroactivity.

The situation is different for TiO₂-[Ru(tpy)(bpy(PO₃H₂)(OH)₂)]²⁺, where use of the Q/H₂Q relay resulted in sustained, but lower, photocurrents with no loss of activity over extended photolysis periods. With hydroquinone as the reducing agent, IPCE values for TiO₂-Ru^{II}-OH₂²⁺ actually increase from less than 0.3% to over 3% as the 0.1 M HClO₄ content was increased from 1% to 5% and to as high as 8% at 30% 0.1 M HClO₄. In fact, photocurrents were immeasurably small unless water was present.

Based on a detailed mechanistic study on the oxidation of hydroquinone (H₂Q) by *cis*-[Ru^{IV}(bpy)₂(py)(O)]²⁺ and *cis*-[Ru^{III}(bpy)₂(py)(OH)]²⁺ in acetonitrile, oxidation of hydroquinone by either occurs by proton-coupled electron transfer (coupled electron-proton transfer (EPT)), eqs 8 and 9, with *k*_{H₂O}/*k*_{D₂O} kinetic isotope effects of 29 for eq 8 and 9.7 for eq 9. In water, the rate constant for oxidation by Ru^{III}-OH₂²⁺ (*k*₂ = 1.1 × 10⁶) is actually slightly larger than oxidation by Ru^{IV}=O²⁺ (*k*₂ = 9.2 × 10⁵) even though Ru^{IV}=O²⁺ is the stronger oxidant by 0.11 eV.²⁴



In the final step, disproportionation of the semiquinone radical yields hydroquinone and benzoquinone as products, eq 10.



The same mechanism presumably occurs on the surface even though there was no significant H₂O/D₂O effect on the IPCE efficiency. An independent study on the reduction of TiO₂-Ru^{IV}=O²⁺ by hydroquinone has shown that diffusion into the microporous film environment is rate determining, which explains the lack of a measurable isotope effect.³⁹

With hydroquinone as reductant, a proposed photoelectrochemical mechanism is shown in Scheme 3. The net reaction is the photochemical dehydrogenation of H₂Q to

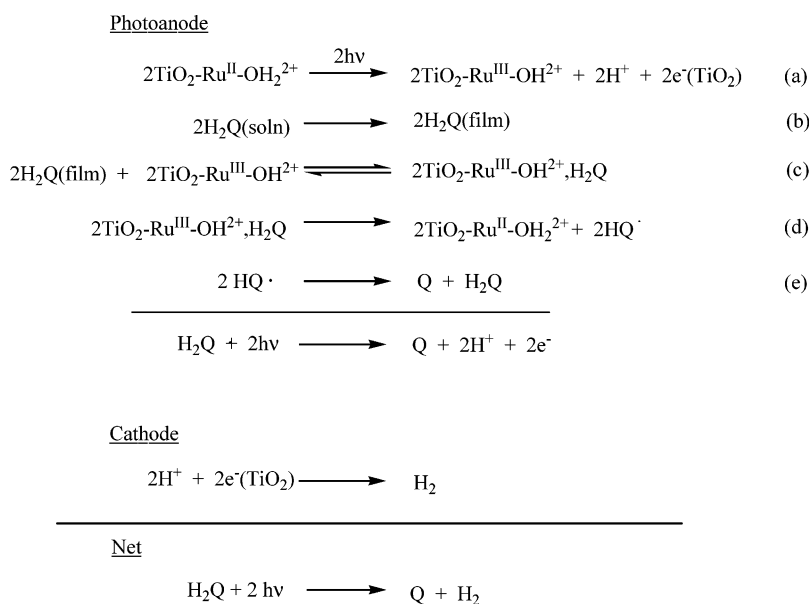
(36) Heimer, T. A.; Bignozzi, C. A.; Meyer, G. J. *J. Phys. Chem.* **1993**, *97*, 11987.

(37) Armadelli, R.; Argazzi, R.; Bignozzi, C. A.; Scandola, F. *J. Am. Chem. Soc.* **1990**, *112*, 7099.

(38) Nakao, M.; Itoh, K.; Watanabe, T.; Honda, K. *Ber. Bunsen-Ges. Phys. Chem.* **1985**, *89*, 134.

(39) Gallagher, L. A. Ph.D. Dissertation, University of North Carolina, Chapel Hill, 2001.

Scheme 3

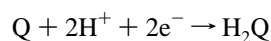


Q. In the photoelectrochemical cell, the reaction is accompanied by a photocurrent and associated photopotential arising from the potential difference between the conduction band of the electrode and the $2\text{H}^+/\text{H}_2$ couple at pH = 1.

The formation of H_2 at the cathode was shown by gas bubble formation, but the amount of gas was not determined quantitatively. In Scheme 3, the photocurrent is initiated by excitation and photoinjection (reaction a). The $[\text{H}_2\text{Q}]$ dependence in Figure 5 can be explained qualitatively as rate limited by diffusion from the external solution into the nanoparticle film at low $[\text{H}_2\text{Q}]$ (reaction b), with film saturation in H_2Q occurring above 0.01 M.

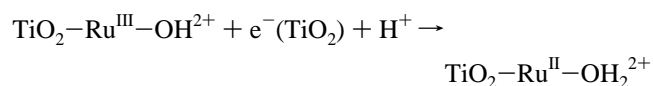
Comparison Between the I_3^-/I^- and the $\text{Q}/\text{H}_2\text{Q}$ Relays.

With added Q at a cathode inert to H_2 formation, the cathode reaction would become

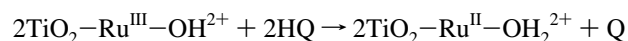
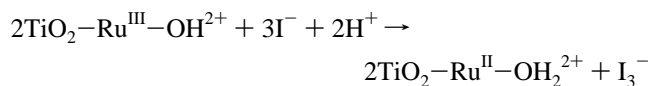


Under these conditions, the photoelectrochemical cell would become a conventional solution photovoltaic cell with the photopotential arising from the potential difference between the TiO_2 conduction band and the $\text{Q}/\text{H}_2\text{Q}$ couple.

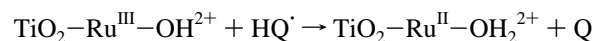
There are some important and revealing comparisons to be made between the I_3^-/I^- and $\text{Q}/\text{H}_2\text{Q}$ couples as redox carriers. Kinetic studies in solution reveal that the reduction of $\text{Ru}^{\text{III}}\text{-OH}^{2+}$ by H_2Q is rapid with $k_2 = 1.1 \times 10^6$.²⁴ Nonetheless, the maximum IPCE value for the I_3^-/I^- couple as compared to the $\text{Q}/\text{H}_2\text{Q}$ couple is greater by a factor of ~ 10 . This observation demonstrates the importance of kinetic effects following photoinjection (reaction a in Scheme 3). In this case, there is a kinetic competition for $\text{TiO}_2\text{-Ru}^{\text{III}}\text{-OH}^{2+}$ between back electron transfer from the photoexcited electrons



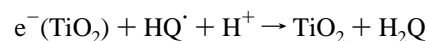
and reduction by I^- or H_2Q



Both reactions must occur by initial one-electron steps and the intervention of one-electron intermediates, I_2^- , $\text{HQ}\cdot$ in reactions such as



Reduction of the semiquinone radical by the photoexcited electron may also contribute to the lower IPCE with hydroquinone.

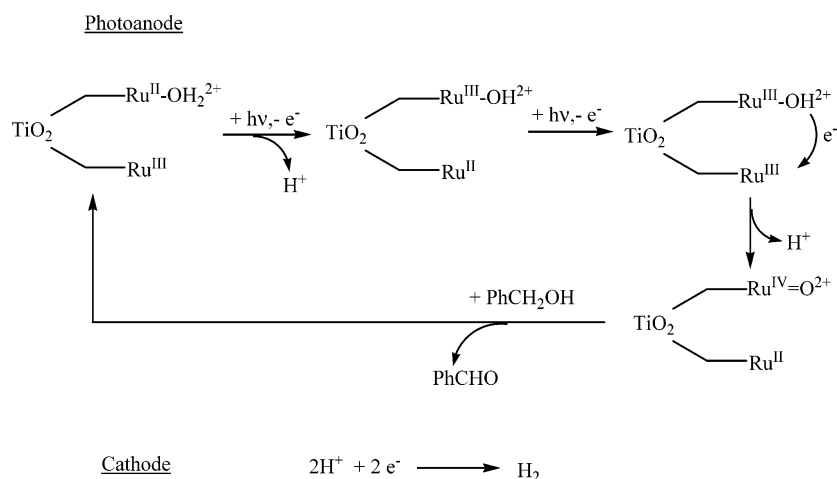


A key difference between I^- and hydroquinone as reductants is presumably a higher affinity of I^- toward the TiO_2 films due to ion-pairing with the cationic $\text{TiO}_2\text{-Ru}^{\text{II}}\text{-OH}_2^{2+}$ sites. Ion-pairing provides the reducing equivalents for Ru^{III} re-reduction at the site where it is produced. Anionic reductants have been suggested as an important element in ensuring the efficiency of dye-sensitized solar cells.⁴⁰

There is a significant difference between the two couples in their response to added water as 0.1 M HClO_4 . For the $\text{Q}/\text{H}_2\text{Q}$ couple, IPCE values increase incrementally up to 5% (the miscibility limit) and up to 30% in acetonitrile. This is a significant effect with IPCEs reaching nearly 10% in acetonitrile with 30% 0.1 M HClO_4 . The enhancement with added water may also be a partitioning effect with the affinity of the interior of the films toward hydroquinone enhanced in solvent mixtures.

(40) Cahen, D.; Hodes, G.; Grätzel, M.; Guillemoles, J. F.; Riess, I. *J. Phys. Chem. B* **2000**, *104*, 2053.

Scheme 4



There is also a significant difference in long-term behavior toward the Q/H₂Q couple between the TiO₂-Ru^{II}-OH₂²⁺ and TiO₂-Ru^{II} electrodes. Photocurrents for the latter decrease markedly as the photolysis period is extended. The origin of this effect is unclear especially given the negative evidence for significant surface change from UV-visible, electrochemical, and XPS measurements.

The surface poisoning effect is not observed for TiO₂-Ru^{II}-OH₂²⁺. This difference in behavior points to a change in mechanism for reduction of Ru^{III} between the two couples at the surface. Reduction of TiO₂-Ru^{III}-OH₂²⁺ by hydroquinone at the surface presumably occurs by coupled electron-proton transfer (EPT) as in eq 9, and the sequence, H₂Q → HQ[•], followed by disproportionation, eq 10. With TiO₂-[Ru^{III}(bpy)₂(bpy(PO₃H₂)₂)]²⁺, the mechanism may involve initial outer-sphere electron transfer and the sequence H₂Q → H₂Q^{•+} → HQ[•] + H⁺. The intermediate H₂Q^{•+} and its interaction with the surface or the surface link to TiO₂-Ru²⁺ may cause surface passivation toward further electron transfer, although the detailed mechanism for this behavior is unknown.

Mixed Surfaces. As noted above, we investigated the IPCE characteristics of mixed surfaces containing [Ru(tpy)-(bpy(PO₃H₂))(OH₂)]²⁺ and [Ru(bpy)₂(bpy(PO₃H₂)₂)]²⁺ on TiO₂ to explore the possible development of an indirect route to highly reactive TiO₂-[Ru^{IV}(tpy)(bpy(PO₃H₂))(O)]²⁺ (TiO₂-Ru^{IV}=O²⁺) by cross-surface electron transfer.

IPCE measurements on the mixed surfaces are consistent with the absence of significant cooperativity between TiO₂-Ru^{II} and TiO₂-Ru^{II}-OH₂²⁺. With I⁻ as reductant, the experimental photocurrents are the normalized sum of separate contributions from TiO₂-Ru^{II}* and TiO₂-Ru^{II}-OH₂²⁺* within experimental error, ±10%. The absence of cooperativity effects is consistent with excitation and photoinjection at the individual TiO₂-Ru^{II}* and TiO₂-Ru^{II}-OH₂²⁺ sites on a time scale that is rapid compared to cross-surface electron and energy transfer.

Energy transfer from TiO₂-Ru^{II}-OH₂²⁺* to TiO₂-Ru^{II} is spontaneous by ~3000 cm⁻¹ based on the absorption and IPCE maxima in Figures 2 and 3. Similarly, cross-surface electron transfer, TiO₂-Ru^{II}-OH₂²⁺ → TiO₂-Ru^{III}, is

favored by 0.24 V (1900 cm⁻¹). On nanoparticle surface films of ZrO₂, both ZrO₂-Ru^{II}* → ZrO₂-Os^{II} energy transfer (ΔG° = -0.4 eV, 3200 cm⁻¹)^{13,41} and ZrO₂-Os^{II} → ZrO₂-Ru^{III} electron transfer³⁵ (ΔG° = -0.4 eV) are facile but orders of magnitude less than the ~picosecond time scale for photoinjection for adsorbed metal complex dyes on TiO₂.⁴²

There is a further manifestation of the lack of cooperativity between TiO₂-Ru^{II} and TiO₂-Ru^{II}-OH₂²⁺ on mixed surfaces. The photoactivity loss with time for TiO₂-Ru^{II} with added hydroquinone was noted above. On mixed surfaces with added H₂Q, the photocurrent decreases with time until TiO₂-Ru^{II} is deactivated. The photocurrent response that remains is stable and is proportional to the mole fraction of TiO₂-Ru^{II}-OH₂²⁺. This points to selective deactivation toward electron transfer at surface-bound Ru^{II} or on the surface in the vicinity of Ru^{II}.

Two-Electron Reductants. The results with hydroquinone are not directly relevant to possible access and utilization of [Ru^{IV}(tpy)(bpy(PO₃H₂))(O)]²⁺ on the surface with more interesting reductants such as those in eqs 6 and 7. Hydroquinone is an unusual reagent in its high relative reactivity toward both Ru^{III}-OH₂²⁺ and Ru^{IV}=O²⁺. As noted above, rate constants for oxidation of H₂Q by the Ru^{III}-OH₂²⁺ and Ru^{IV}=O²⁺ forms of *cis*-[Ru(bpy)₂(py)(OH₂)]²⁺ are comparable.¹⁴ The oxidation of benzyl alcohol to benzaldehyde is far slower. It occurs by a two-electron mechanism, and reactivity with Ru^{IV}=O²⁺ is highly favored kinetically over Ru^{III}-OH₂²⁺.^{11,28} This creates a challenge for the use of one-proton, one-electron-transfer mechanisms for carrying out two-electron reactions. Excitation and injection on TiO₂-Ru-OH₂²⁺ surfaces produce Ru^{III}-OH₂²⁺, eq 11, but TiO₂-Ru^{IV}=O²⁺ is inaccessible because TiO₂-Ru^{III}-OH₂²⁺ is nearly transparent in the visible.

In principle, mixed surfaces containing both chromophores and catalytic sites offer a solution to this problem. The mechanisms for accessing the catalytically active form,

(41) Trammell, S. A.; Yang, J. C.; Sykora, M.; Fleming, C. N.; Odobel, F.; Meyer, T. J. *J. Phys. Chem. B* **2001**, *105*, 8895–8904.

(42) Kelly, C. A.; Meyer, G. J. *Coord. Chem. Rev.* **2001**, *211*, 295–315 and references therein.

Design of Photoelectrochemical Synthesis Cells

$\text{TiO}_2\text{-Ru}^{\text{IV}}=\text{O}^{2+}$, based on excitation, injection, and cross-surface electron transfer are shown in Scheme 4 for the dehydrogenation of benzyl alcohol. The initial formation of $\text{TiO}_2\text{-Ru}^{\text{III}}\text{-OH}^{2+}$ could occur by direct or indirect mechanisms. Subsequent excitation and injection by $\text{TiO}_2\text{-Ru}^{\text{II}}$ followed by cross-surface electron transfer would form $\text{TiO}_2\text{-Ru}^{\text{IV}}=\text{O}^{2+}$.

Initial experiments on mixed surfaces with benzyl alcohol as the reductant reveal that photocurrents are too low to be of interest. The challenge with such reductants will be to

adsorb more reactive oxidants on the surface. With more reactive oxidants, the mechanism shown in Scheme 4 may become viable.

Acknowledgment. Funding for this work was provided by the Department of Energy (grant no. DE-FG02-96-ER14607) and Los Alamos National Laboratory (Laboratory Directed Research and Development Program Project 20020222).

IC0400991